DEVELOPMENTAL DYNAMICS 246:539–549, 2017
DOI: 10.1002/DVDY.24512

Identification of Target Genes Downstream of Semaphorin6A/PlexinA2 Signaling in Zebrafish

Sarah E. Emerson,[1] Riley M. St. Clair,[1] Ashley L. Waldron,[1] Sierra R. Bruno,[1] Anna Duong,[1] Heather E. Driscoll,[2] Bryan A. Ballif,[1] Sarah McFarlane,[3] and Alicia M. Ebert [1]*

[1]Department of Biology, University of Vermont, Burlington, Vermont
[2]Vermont Genetics Network Bioinformatics Core and Department of Biology, Norwich University, Northfield, Vermont
[3]Department of Cell Biology and Anatomy, Hotchkiss Brain Institute, University of Calgary, Calgary, Alberta, Canada

Background: Semaphorin (Sema)/Plexin (Plxn) signaling is important for many aspects of neuronal development, however, the transcriptional regulation imposed by this signaling pathway is unknown. Previously, we identified an essential role for Sema6A/PlxnA2 signaling in regulating proliferation and cohesion of retinal precursor cells (RPCs) during early eye development. This study used RNA isolated from control, Sema6A-deficient and PlxnA2-deficient zebrafish embryos in a microarray analysis to identify genes that were differentially expressed when this signaling pathway was disrupted. **Results:** We uncovered a set of 58 transcripts, and all but 1 were up-regulated in both *sema6A* and *plxnA2* morphants. We validated gene expression changes in subset of candidates that are suggested to be involved in proliferation, migration or neuronal positioning. We further functionally evaluated one gene, *rasl11b*, as contributing to disrupted proliferation in *sema6A* and *plxna2* morphants. Our results suggest *rasl11b* negatively regulates proliferation of RPCs in the developing zebrafish eye. **Conclusions:** Microarray analysis has generated a resource of target genes downstream of Sema6A/PlxnA2 signaling, which can be further investigated to elucidate the downstream effects of this well-studied neuronal and vascular guidance signaling pathway. *Developmental Dynamics 246:539–549, 2017.* © 2017 Wiley Periodicals, Inc.

Key words: retina; eye development; rasl11b; microarray; proliferation; rx3:GFP

Submitted 22 November 2016; First Decision 10 March 2017; Accepted 8 April 2017; Published online 25 April 2017

Introduction

Neuronal migration and positioning are important aspects of nervous system development. During the early stages of neuronal development, guidance cues are essential to lead neurons and their processes to correct target tissues. One well-studied group of guidance cues are the Semaphorins (Semas). Semas are a family of transmembrane and secreted proteins that typically signal through Plexin (Plxn) receptors. There are eight subclasses of Semas. Semas 1 and 2 are found in invertebrates, 3–7 are found in vertebrates, and Sema V is found in the genome of nonneurotropic DNA viruses (Neufeld and Kessler, 2008). The Plexin family is composed of two invertebrate Plxns, A and B, and four classes of vertebrate Plxns, A1-4, B1-3, C1, and D1 (Tamagnone et al., 1999). Semas and Plxns have tissue-specific expression patterns, and many Semas can signal through multiple Plxn family members. Semas were initially discovered with respect to their role as repulsive guidance cues for migrating axons (Luo et al., 1993), although it is now appreciated that they have much broader roles in development. They have been implicated in vasculogenesis (Serini et al., 2003), tumorigenesis (Neufeld and Kessler, 2008), immunity (Shi et al., 2000), and bone development (Behar et al., 1996). Here, we focus specifically on the interaction and downstream effects of Sema6A and PlxnA2 in early eye development.

During eye development, retinal precursor cells (RPCs) are directed from the optic stalk into the correct domain of the developing retina (Rembold et al., 2006). We previously demonstrated that Sema6A and its receptor, PlxnA2, are necessary for the proliferation and cohesion of RPCs within the early embryonic eye vesicles (Ebert et al., 2014). More recently, Sema6A and PlxnA2 were shown to be required for interkinetic nuclear migration of RPCs within optic vesicles (Belle et al., 2016). In addition, Sema6/PlxnA signaling is required for neuronal positioning in the cerebellum (Renaud et al., 2008; Renaud and Chedotal, 2014), lamination of the hippocampus (Tawarayama et al., 2010), and

ABBREVIATIONS: ANOVA, analysis of variance; BH, Benjamini and Hochberg; *dcdc2b*, doublecortin domain-containing 2b; DIG, digoxigenin; ECM, extracellular matrix; GAP, GTPase activating protein; GEF, guanine nucleotide exchange factor; GFP, green fluorescent protein; hpf, hours post fertilization; logFC, log-fold change; MAPK, mitogen-activated protein kinase; *mmp*, matrix metalloproteinase; MO, morpholino; PBST, (phosphate buffered saline + 1% Triton; pHH3, phospho-Histone H3; Plxn, plexin; *rasl11b*, RAS-like, family 11, member B; *rbl2*, retinoblastoma-like protein 2; RMA, robust multichip average; RPCs, retinal precursor cells; RT-PCR, reverse transcriptase-polymerase chain reaction; Sema, semaphorin; *shtn-1*, Shootin-1

Grant sponsor: U.S. National Science Foundation; Grant number: IOS1456846; Grant sponsor: Foundation Fighting Blindness Canada.
*Correspondence to: Alicia M. Ebert, Department of Biology, University of Vermont, Burlington, VT 05405. E-mail: amebert@uvm.edu

Article is online at: http://onlinelibrary.wiley.com/doi/10.1002/dvdy.24512/abstract

guidance of the corticospinal tract (Rünker et al., 2008), among other roles. Several studies have begun to uncover the intracellular signaling mechanisms downstream of activated PlxnA receptors (Oinuma et al., 2004; Toyofuku et al., 2005; He et al., 2009); however, before this study, it was unknown what transcriptional regulation occurred downstream of Sema6A/PlxnA2 signaling.

Microarray analysis using RNA extracted from 18 somite zebrafish embryos deficient in either Sema6A or PlxnA2 has enabled the identification of several downstream transcriptional targets of Sema6A/PlxnA2 signaling during early stages of neuronal development. Further characterization of one of these genes, RAS-like, family 11, member B (*rasl11b*), revealed its role in regulating RPC proliferation.

Results and Discussion

Microarray Analysis Identifies Transcriptional Changes Downstream of Sema6A/PlxnA2 Signaling

Confirming our previous results (Ebert et al., 2014), morpholino antisense oligonucleotides (MOs) targeted to either *sema6A* or *plxnA2* resulted in decreased proliferation and cohesion of RPCs within migrating optic vesicles compared with control embryos. To observe these phenotypes, we used the *rx3*:GFP zebrafish transgenic line that expresses green fluorescent protein (GFP) in RPCs and the hypothalamus (Rembold et al., 2006). Using confocal microscopy, we identified GFP-positive RPCs outside of the eye field and optic vesicles that were closer together in morphant embryos (Fig. 1A–F). Using a mitotic marker, phospho-Histone H3 (pHH3), we observed less proliferation within the GFP-positive optic vesicles (Fig. 1A–C,L; control 100%, N = 3, n = 30; *plxnA2* MO 25.11% ± 0.72 N = 3, n = 30, $P < 0.0001$; *sema6A* MO 28.86% ± 1.12, N = 3, n = 30; $P < 0.0001$, one-way analysis of variance [ANOVA], multiple comparisons test).

As these embryos develop further, the decreased proliferation results in smaller eyes at 48 hr post fertilization (hpf) (Fig. 1G,H,J,M; eye diameter relative to head length; Control 0.49 μm ± 0.008 μm, N = 3, n = 30; *plxnA2* MO 0.40 μm ± 0.01 μm, N = 3, n = 29, $P < 0.0001$; *sema6A* MO 0.42 μm ± 0.009 μm, N = 3, n = 31, $P < 0.0001$, one-way ANOVA, Multiple comparisons test). Off-target effects and specificity of both *sema6A* and *plxnA2* morpholinos have been addressed with secondary non-overlapping morpholino constructs, partial rescue of phenotypes by means of full-length mRNA injections, and penetrance verified by the absence of wildtype gene products by reverse transcriptase-polymerase chain reaction (RT-PCR) (Ebert et al., 2014). To re-address morpholino specificity in this study, co-injections of morpholino with full-length human *SEMA6A* or *PLXNA2* mRNA partially rescued eye size (Fig. 1I,K,M; eye diameter relative to head length; control 0.49 μm ± 0.008 μm, N = 3, n = 30; *PLXNA2* rescue 0.45 μm ± 0.009 μm, N = 3, n = 32, $P < 0.001$; *SEMA6A* rescue 0.48 μm ± 0.008 μm, N = 3, n = 28, $P < 0.001$; one-way ANOVA, multiple comparisons test).

Overexpression of *SEMA6A* or *PLXNA2* human mRNA alone exhibited no significant developmental phenotypes (data not shown). Considering that eye development takes several hours, we wanted to investigate what transcriptional changes were occurring downstream of Sema6A/PlxnA2 signaling that could be controlling this process. We compared gene expression levels of 18 somite *plxnA2* morphants compared with uninjected control embryos (Fig. 2A) and 18 somite *sema6A* morphants compared with uninjected control embryos (Fig. 2B). In a microarray of 4885 zebrafish genes, we identified 58 significantly (greater than two-fold) differentially regulated genes that were in common to both morphants (Table 1, 2C, GEO accession# GSE86246). Strikingly, of the 58 genes, 57 were up-regulated and only 1 was down-regulated, suggesting that Sema6A/PlxnA2 signaling is largely repressive to downstream transcriptional targets (Figs. 2C, 3). Using gene ontology information, we prioritized genes predicted to be involved in cell migration and proliferation for validation and further functional studies due to the phenotypes observed in morphant embryos.

In Situ Hybridization and RT-PCR Validation of Microarray Results

Zebrafish embryos were injected with either *sema6A* or *plxnA2* morpholinos at the one cell stage, and fixed at the 18 somite stage, dehydrated, and processed for in situ hybridization. Digoxigenin (DIG)-labeled antisense riboprobes were generated for RAS-like, family 11, member B *(rasl11b)*, shootin-1 *(shtn-1)*, doublecortin domain-containing 2b (*dcdc2b)*, matrix metalloproteinase 2 *(mmp2)*, and retinoblastoma-like protein 2 *(rbl2)*, and in situ hybridization was performed on control and morphant embryos. Probe intensity for all five candidate genes was consistent with microarray results and offered additional spatial information (Fig. 4A–E). Transverse sections of *rasl11b* and *shtn-1* labeled embryos show neuronal expression, including in the developing eye, at this early stage (Fig. 4A,B, right columns).

We observed overlap between previously reported *plxnA2* and *sema6A* expression (Ebert et al., 2014) and the candidate genes, supporting a relationship between Sema6A/PlxnA2 signaling and these genes. We generated cDNA from uninjected control, *sema6A* morphant, and *plxnA2* morphant embryos at 18 somites and performed RT-PCR (Fig. 4A′–E′). The results are consistent with the microarray and in situ expression data, showing increases in transcriptional levels of the candidate genes in both morphants compared with uninjected control (Fig. 4A′–E′; *rasl11b* control 0.1137 ± 0.04, N = 3; *sema6A* MO 0.34 ± 0.02, N = 3, $P < 0.01$; *plxnA2* MO 0.32 ± 0.01, N = 3, $P < 0.01$; *shtn-1* control 0.08 ± 0.01, N = 3; *sema6A* MO 0.28 ± 0.01, N = 3, $P < 0.01$; *plxnA2* MO 0.24 ± 0.03, N = 3, $P < 0.01$; *dcdc2b* control 0.06 ± 0.004, N = 3; *sema6A* MO 0.13 ± 0.02, N = 3, $P < 0.05$; *plxnA2* MO 0.24 ± 0.02, N = 3, $P < 0.001$; *mmp2* control 0.004 ± 0.001, N = 5; *sema6A* MO 0.21 ± 0.07, N = 5, $P < 0.05$; *plxnA2* MO 0.27 ± 0.06, N = 5, $P < 0.01$; *rbl2* control 0.01 ± 0.002, N = 4; *sema6A* MO 0.17 ± 0.02, N = 4, $P < 0.001$; *plxnA2* MO 0.15 ± 0.03, N = 4, $P < 0.01$; one-way ANOVA, multiple comparisons test).

Overexpression of rasl11b Leads to Decreased Proliferation in Optic Vesicles

Microarray results indicated that *rasl11b* has a 2.18 log-fold change (logFC) in *sema6A* morphants and a 1.58 logFC in *plxnA2* morphants (Table 1). We chose to further investigate this gene because of its predicted role in cell proliferation and expression in the developing eye field (Fig. 4A, right column). To determine if increased *rasl11b* expression contributes to decreased proliferation of RPCs, we injected full-length zebrafish *rasl11b* mRNA into single-cell embryos. We visualized proliferation (pHH3) in the early eye field (*rx3*:GFP) of 18 somite embryos injected with

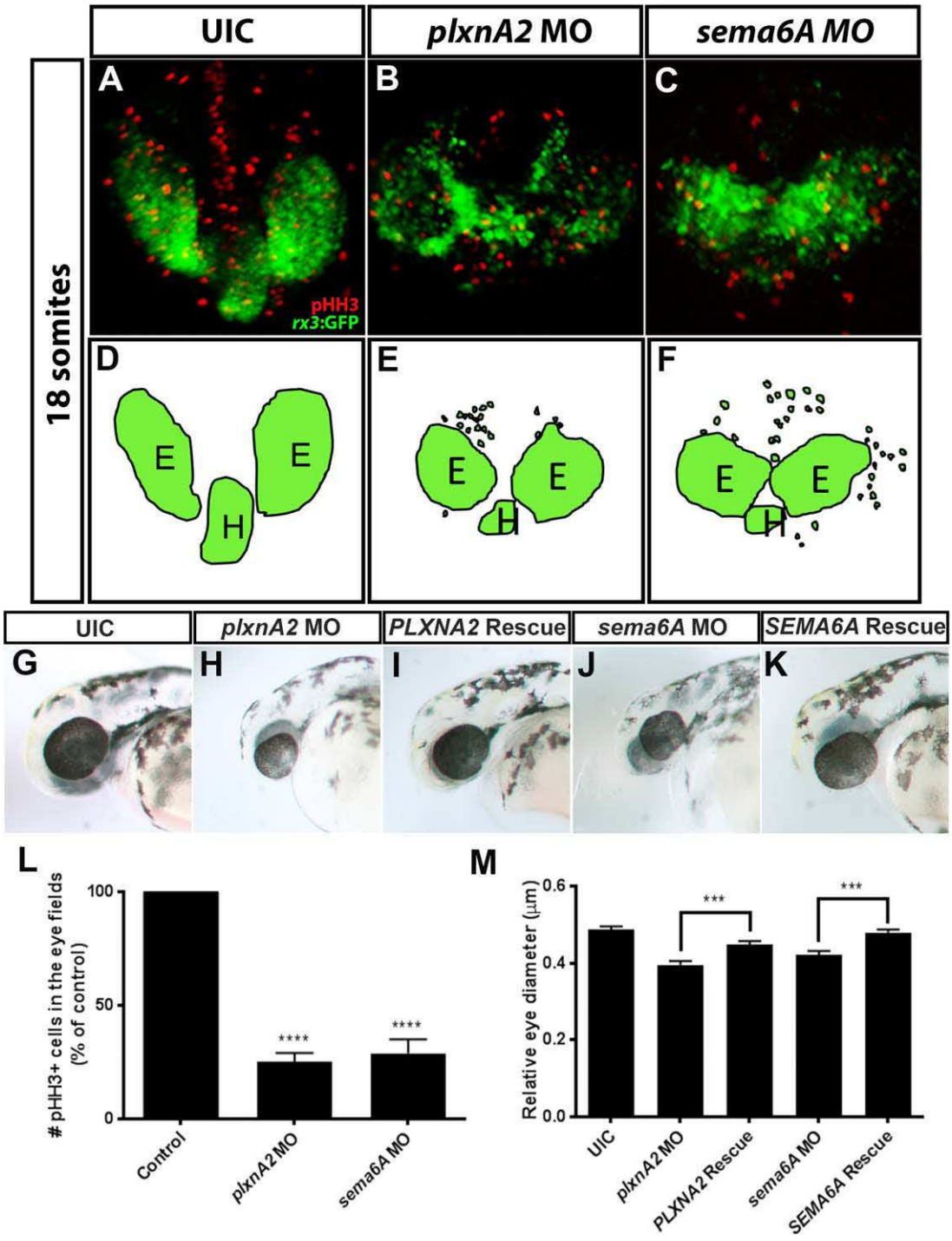

Fig. 1. Sema6A and plxnA2 knockdown leads to loss of cohesion and decreased proliferation in eye vesicles. **A–C:** Confocal dorsal views of 18 somite stage rx3:GFP embryos co-labeled with pHH3. **L:** Both sema6A and plxnA2 morphants display ectopic retinal precursor cells outside of the eye field as well as significantly reduced pHH3 positive cells in the developing eyes compared with controls, as quantified (control 100%, N = 3, n = 30; plxnA2 MO 25.11% ± 0.72%, N = 3, n = 30, ****$P < 0.0001$; sema6A MO 28.86% ± 1.12%, N = 3, n = 30; ****$P < 0.0001$, one-way ANOVA, multiple comparisons post-hoc test). **D–F:** Schematics of rx3:GFP dorsal view. **G,H,J,M:** Decreased proliferation is later observed as smaller eyes at 48 hpf (control 0.49 μm ± 0.008 μm, N = 3, n = 30; plxnA2 MO 0.40 μm ± 0.01 μm, N = 3, n = 29, ****$P < 0.0001$; sema6A MO 0.42 μm ± 0.009 μm, N = 3, n = 31; ****$P < 0.0001$, one-way ANOVA, multiple comparisons test). G,I,K,M: Full length human PLXNA2 and SEMA6A mRNA partially rescues smaller eye phenotypes (control 0.49 μm ± 0.008 μm, N = 3, n = 30; PLXNA2 rescue 0.45 μm ± 0.009 μm, N = 3, n = 32, ***$P < 0.001$; SEMA6A rescue 0.48 μm ± 0.008 μm, N = 3, n = 28; ***$P < 0.001$, one-way ANOVA, multiple comparisons test. Error bars indicate SEM). E, eye; H, hypothalamus.

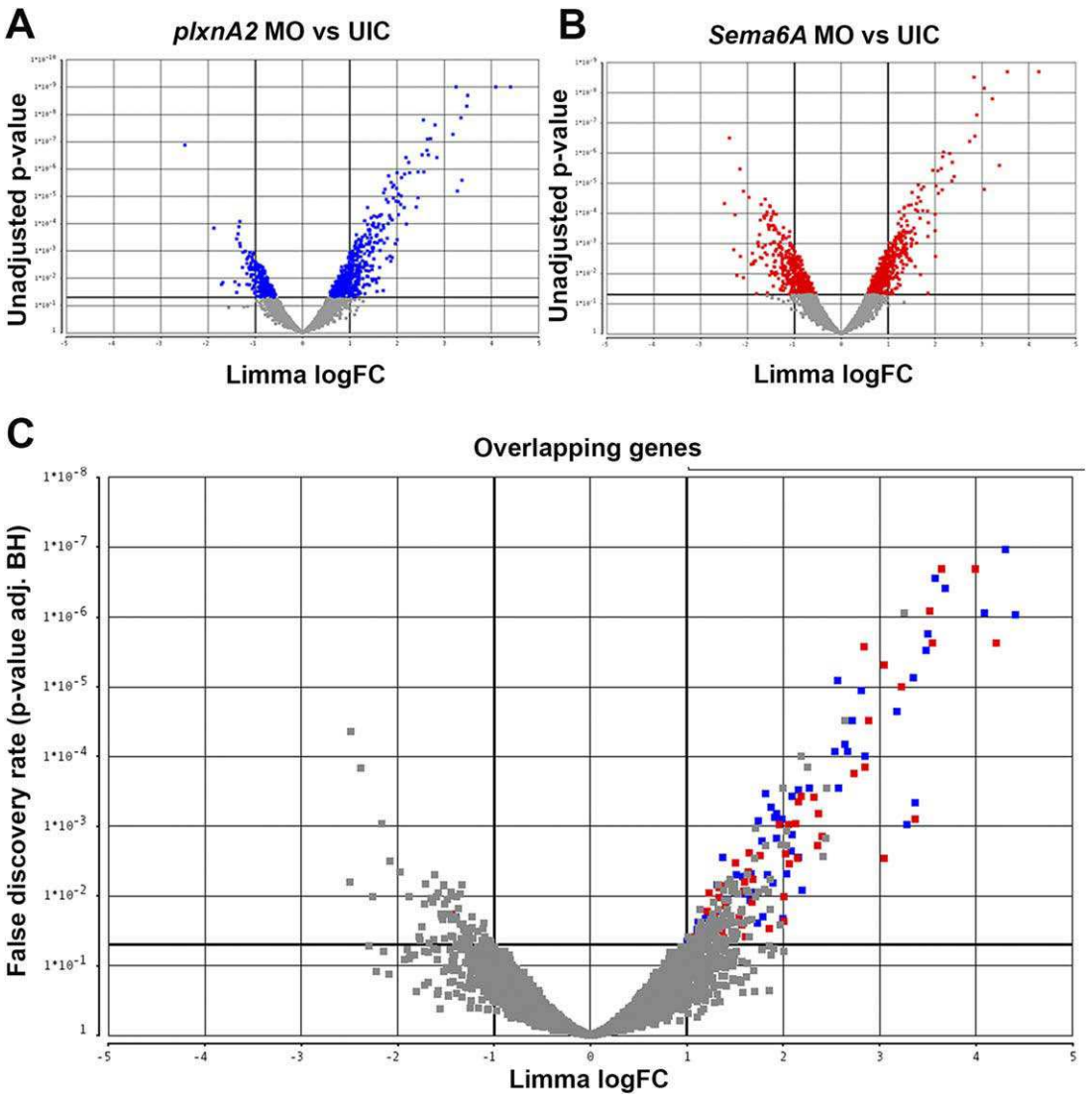

Fig. 2. Volcano plots denoting differential gene expression. Each point represents a gene in the microarray. **A:** Gene expression changes between plxnA2 MO and uninjected controls (UIC). **B:** sema6A MO compared with UIC. Gray are nonsignificant. **C:** Overlapping genes in both plxnA2 and sema6A plots. Blue squares indicate significantly different expression levels in plxnA2 MO-UIC, red squares in sema6A MOUIC. Gray are nonsignificant in at least one condition, with under a two-fold change difference in expression or $P > 0.05$.

200 pg or 400 pg *rasl11b* mRNA. Overexpression of *rasl11b* resulted in decreased RPC proliferation in a dose-dependent manner (Fig. 5A–D; control 100%, N = 3, n = 30; 200 pg *rasl11b* 72.87% ± 4.25%, N = 3, n = 38, $P < 0.0001$; 400 pg *rasl11b* 62.19% ± 4.01%, N = 3, n = 31, $P < 0.0001$; one-way ANOVA, multiple comparisons test). At 48 hpf, overexpression of *rasl11b* resulted in smaller eyes (Fig. 5E–G; eye diameter relative to head length; control 0.48 μm ± 0.005 μm, N = 3, n = 30; 400 pg *rasl11b* 0.39 μm ± 0.01 μm, N = 3, n = 36, $P < 0.0001$; one-way ANOVA, multiple comparisons test). We show that *rasl11b* is negatively regulated downstream of Sema6A/PlxnA2 signaling and when overexpressed, decreases RPC proliferation and eye size.

Proposed Signaling Mechanism of rasl11b Impinging on Ras Signaling

Rasl11b is a small atypical GTPase that has been implicated in prostate cancer (Louro et al., 2004). In zebrafish, Rasl11b inhibits mesendodermal and prechordal plate formation during embryogenesis, and interacts with the one-eyed pinhead signaling pathway (Pezeron et al., 2008). Rasl11b is highly conserved in vertebrates and is atypical to most Ras-like family members in two ways. First, it is cytosolic and lacks carboxy terminal lipid modification sites which allow for membrane anchoring (Pezeron et al., 2008). Second, it has a lower GTPase activity than Ras, and is more often in its active GTP-bound state (Colicelli, 2004). Ras proteins are well known to be involved in the mitogen-activated protein kinase (MAPK) pathway, therefore, we hypothesize that Rasl11b acts as a negative regulator of MAPK by outcompeting Ras for its effectors such as Raf, leading to decreases in RPC proliferation seen in morphant embryos.

It is known that Plexins have an intracellular split GAP (GTPase activating protein) domain that can regulate Ras-family small GTPases (Negishi et al., 2005; Pasterkamp, 2005). Small GTPases act as molecular switches: “on” when GTP-bound, and “off” when GDP-bound (Bos et al., 2007). GAPs increase GTP

TABLE 1. List of 58 genes that are differentially regulated downstream of Sema6a/PlxnA2 signaling at 18 somites, common to both morphants compared to uninjected controls. GEO accession # GSE86246

zfin symbol	ensembl gene ID	logFC Sema-UIC	logFC Plexin-UIC
ace	ENSDARG00000079166	2.02	2.67
ankrd50	ENSDARG00000007077	1.59	1.99
atf5a	ENSDARG00000068096	2	2
atp1b4	ENSDARG00000053262	-1.44	-1.4
atxn1b	ENSDARG00000060862	3.99	4.3
azin1a	ENSDARG00000052789	1.36	1.6
baxa	ENSDARG00000020623	1.35	1
bbc3	ENSDARG00000069282	2.37	3.35
caprin2	ENSDARG00000020749	1.36	1.29
casp8	ENSDARG00000058325	3.55	3.5
cd40	ENSDARG00000054968	1.57	2.84
cdkn1a	ENSDARG00000076554	2.13	2.53
cdkn2a	ENSDARG00000037262	3.05	3.28
cica	ENSDARG00000071150	1.28	1.88
crygn1	ENSDARG00000087437	2.31	2.27
cxcr3.3	ENSDARG00000070669	1.09	1.51
dcdc2b	ENSDARG00000053744	1.25	2.16
dgki	ENSDARG00000063578	1.55	1.55
exo5	ENSDARG00000042727	3.22	3.48
fos	ENSDARG00000031683	3.05	2.81
fosl1	ENSDARG00000015355	2.4	2.03
ftr85	ENSDARG00000034707	1.5	2.09
gadd45aa	ENSDARG00000043581	2.85	3.18
gig2p	ENSDARG00000088260	1.23	1.32
gpd1a	ENSDARG00000043701	1.64	1.74
gpr61	ENSDARG00000003900	1.85	2.2
gtpbp1l	ENSDARG00000042900	2.84	2.56
igf2a	ENSDARG00000018643	1.51	1.82
lnx1	ENSDARG00000043323	1.4	1.41
lygl1	ENSDARG00000056874	1.38	1.66
mat2al	ENSDARG00000063665	2.89	2.64
mdm2	ENSDARG00000033443	1.76	1.91
metrnl	ENSDARG00000007289	1.67	1.71
mfap4	ENSDARG00000090557	2.73	4.09
mmp2	ENSDARG00000017676	1.33	1.31
ms4a17a.2	ENSDARG00000093546	1.61	1.73
nebl	ENSDARG00000021200	2	1.79
nupr1	ENSDARG00000094300	1.64	1.93
parp3	ENSDARG00000003961	1.96	1.77
phlda2	ENSDARG00000042874	1.28	1.63
pmaip1	ENSDARG00000089307	2.15	1.89
phlda3	ENSDARG00000037804	3.64	3.57
ppm1e	ENSDARG00000026499	1.06	1.1
prox2	ENSDARG00000041952	1.69	1.67
rasl11b	ENSDARG00000015611	2.18	1.58
rb12	ENSDARG00000045636	3.52	3.68
rd3	ENSDARG00000031600	1.21	1.93
rev1	ENSDARG00000018296	1.6	1.41
mf169	ENSDARG00000042825	2.05	2.71
rps27l	ENSDARG00000090186	2.06	2.08
rpz5	ENSDARG00000075718	3.37	3.37
sesn1	ENSDARG00000020693	1.49	2.57
shtn1	ENSDARG00000039697	1.21	1.12
tnfaip6	ENSDARG00000093440	1.33	1.19
tnfrsf27	ENSDARG00000079403	4.21	4.4
tp53	ENSDARG00000035559	1.23	1.37
upb1	ENSDARG00000011521	2.16	2.09

hydrolysis and thereby increase the "off," GDP-bound form of the protein. Plxn intracellular GAP domains are inactive when Plxns are in inactive, open conformations. Upon Sema binding, PlxnAs undergo a conformational change, which forms an active GAP domain, in addition to activating downstream effector proteins (He et al., 2009). When Sema6A/PlxnA2 signaling is disrupted, *rasl11b* expression increased (Table 1; Fig. 4A). We propose that when nonmembrane bound Rasl11b is present, it inhibits membrane-tethered Ras signaling through its lower GTPase activity and its ability to recruit either Raf or the small Ras activating guanine nucleotide exchange factor (GEF), son of sevenless (SOS), away from the membrane. This could sequester Raf or SOS away from Ras, therefore, Ras is predominantly found in its GDP-bound state, reducing signal propagation, and resulting in decreased pro-proliferative effects of the MAPK signaling cascade.

Proposed Contributions of shtn-1, dcdc2b, rbl2, and mmp2 to Morphant Phenotypes

Additional validated genes may also contribute to morphant phenotypes. Microarray results demonstrated that *shtn-1* has a 1.21 logFC in *sema6A* morphants and a 1.12 logFC in *plxnA2* morphants. Shtn-1 is involved in the formation of cellular asymmetric polarization signals, which direct the cell during migration, as seen in the orientation of neurite outgrowth of cultured hippocampal neurons (Toriyama et al., 2006). To polarize, cells need to have carefully regulated amounts of Shtn-1. Overexpression of Shtn-1 in rat hippocampal neurons leads to its impaired asymmetric distribution and induces the formation of surplus axons (Toriyama et al., 2006). Alternatively, Shtn-1 may control the actin cytoskeleton in migrating cells, in that Shtn-1 couples f-actin retrograde flow to L1-CAM aiding with "clutch engagement" at the leading edge of the extending axons of rat hippocampal neurons in culture (Shimada et al., 2008). Thus, we hypothesize that an increase in Shtn-1 could impair the coordinated migration of RPCs, as individual cells fail to either receive the correct polarization signals and/or regulate their actin cytoskeleton.

Dcdc2b has a 1.25 logFC in *sema6a* and a 2.16 logFC in *plxnaA2* morphants (Table 1). It is one of a family of 11 DCX domain-containing proteins. DCX domain-containing proteins are atypical microtubule-associated proteins. They bind to tubulin by means of their DCX domains to regulate microtubule stabilization and also couple microtubule-actin binding through various accessory proteins (Dijkmans et al., 2010). In zebrafish, mutations in *dcdc2b* have uncovered a role in the function of microtubules within cilia of hair cells, correlating with deficits that lead to deafness in humans (Grati et al., 2015). It is known that cytoskeletal microtubule dynamics at the trailing edge of migratory cells are critical for cellular movement, in addition to generating cellular polarity, both of which guide the direction of migration (Ganguly et al., 2012). We hypothesize that the increase in expression of *dcdc2b* in *sema6A* and *plxnA2* morphants is partially responsible for the abnormal RPC migration seen within optic vesicles. Increases in *dcdc2b* could stabilize microtubules, inhibiting microtubule depolymerization at the trailing edge of migrating RPCs. Stabilization would potentially not only slow normal cellular migration, but disrupt the normal direction of migration, and explain why RPCs within morphant optic vesicles do not migrate as a tightly unified group.

Rbl2, sometimes referred to as p130, is a member of the pocket protein family, along with p107 and retinoblastoma (Rb) (Cobrinik, 2005). Mutations to the *Rb* family of genes can lead to a rare

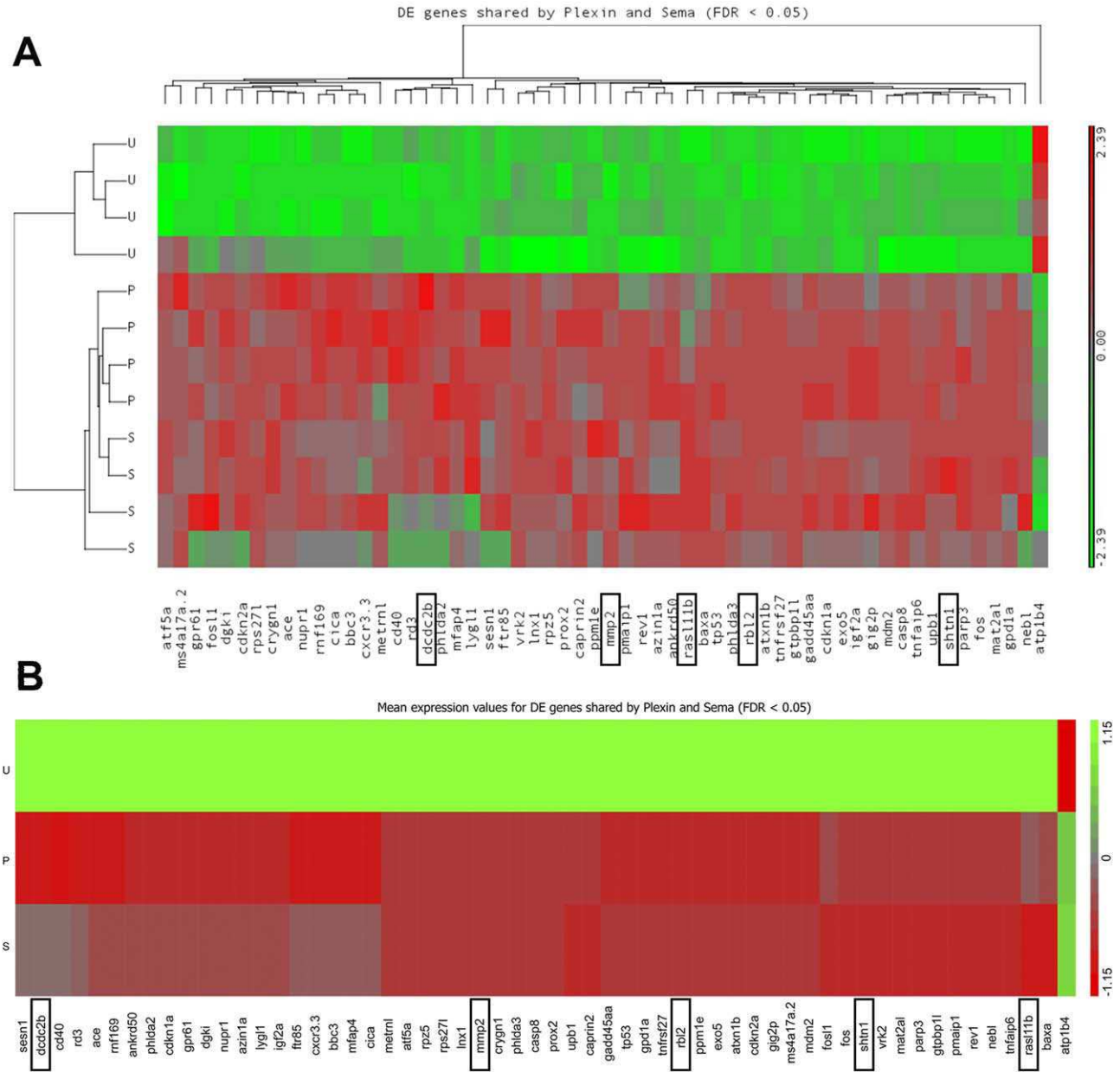

Fig. 3. Microarray heat map of 58 differentially regulated genes in common to both sema6A MO-UIC and plxnA2 MO-UIC. Differential expression is represented on a green to red scale with expression values standardized to a mean of zero and standard deviation of one. **A:** Results from each of the four replicates are shown. **B:** Average expression change of four replicates. Boxes indicate validated genes. U, uninjected control; S, sema6A MO; P, plxnA2 MO.

form of retinal cancer, retinoblastoma, in which cell cycle regulation is lost (Murphree and Benedict, 1984; Friend et al., 1986). Rbl2 has a 3.52 logFC in *sema6a* and a 3.68 logFC in *plxnaA2* morphants (Table 1). These proteins are known to bind to members of the E2F family of transcription factors to regulate the cell cycle. Rbl2 binds to E2F4 to form a repressor complex in mitotic cells to block cell cycle progression (Dingar et al., 2012). The ability of Rbl2 to repress transcription is in part because it can recruit methyltransferases to histones, causing chromatin condensation, and, therefore, decreasing the accessibility of transcriptional machinery to the promoters of genes that promote the cell cycle (Lai et al., 2001). We, therefore, hypothesize that increases in *rbl2* levels in morphant embryos contributes to impaired proliferation of RPCs by blocking the cell cycle.

Matrix metalloproteinases (MMP) are well known for their role in central nervous system development and amphibian regeneration through their ability to degrade extracellular matrix (ECM) proteins (Brinckerhoff and Matrisian, 2002). *mmp2* has a 1.33 logFC in *sema6a* and a 1.31 logFC in *plxnaA2* morphants (Table 1). Recently, *mmp2* was shown to be important for degrading nonpermissive ECM to allow for zebrafish retinal ganglion cell axon outgrowth during recovery from injury (Lemmens et al., 2016). Increases in MMP2 could lead to increased degradation of the ECM surrounding RPCs, and removal of key proteins required

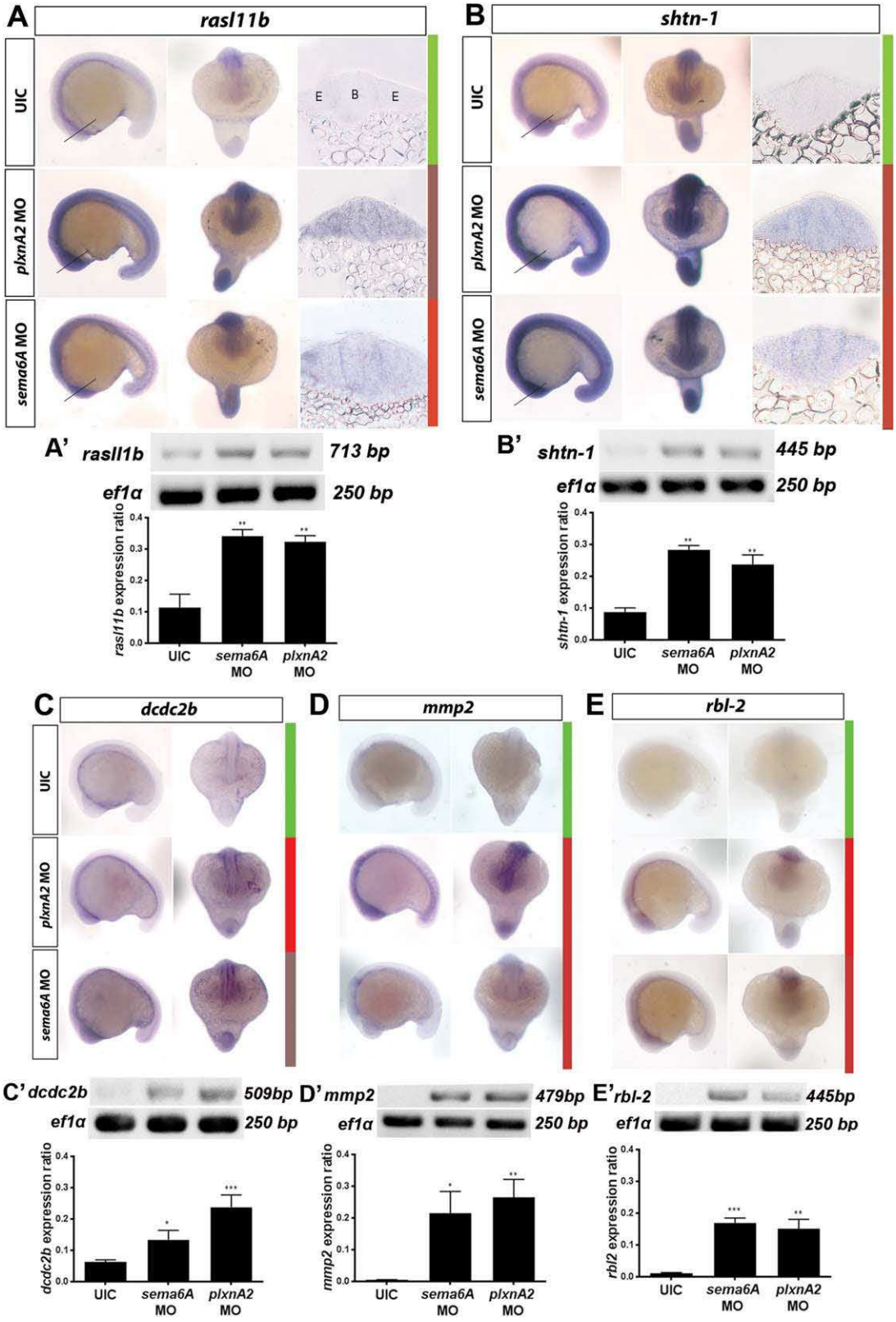

Fig. 4. Microarray validation. In situ hybridization and RT-PCR validation of differential gene expression in plxnA2 and sema6A morphants at 18 somites. **A–E:** Top, middle, and bottom panels show uninjected control, plxnA2 MO injected, and sema6A MO injected embryos, respectively. Left and right panels show lateral and dorsal views, respectively, for each probe under each condition. Colored bars show corresponding heat map expression changes for each gene. UIC, uninjected control. A,B: Additional right panels show transverse 20 μm sections through 18 somite stage brain and eye vesicles processed for in situ hybridization with rasl11b and shtn-1 probes. Lines in whole-mounts indicate corresponding section locations. **A′–E′:** RT-PCR gels and quantification of gene expression changes for each gene as a ratio to ef1α control levels (rasl11b control 0.1137 ± 0.04, N = 3, rasl11b sema6A MO 0.34 ± 0.02, N = 3, $^{**}P < 0.01$; rasl11b plxnA2 MO 0.32 ± 0.01, N = 3, $^{**}P < 0.01$; shtn-1 control 0.08 ± 0.01, N = 3, shtn-1 sema6A MO 0.28 ± 0.01, N = 3, $^{**}P < 0.01$; shtn-1 plxnA2 MO 0.24 ± 0.03, N = 3, $^{**}P < 0.01$; dcdc2b control 0.06 ± 0.004, N = 3, dcdc2b sema6A MO 0.13 ± 0.02 N = 3, $^{*}P < 0.05$; dcdc2b plxnA2 MO 0.24 ± 0.02, N = 3, $^{***}P < 0.001$; mmp2 control 0.004 ± 0.001, N = 5, mmp2 sema6A MO 0.21 ± 0.07, N = 5, $^{*}P < 0.05$; mmp2 plxnA2 MO 0.27 ± 0.06, N = 5, $^{**}P < 0.01$; rbl2 control 0.01 ± 0.002, N = 4, rbl2 sema6A MO 0.17 ± 0.02, N = 4, $^{***}P < 0.001$; rbl2 plxnA2 MO 0.15 ± 0.03, N = 4, $^{**}P < 0.01$; one-way ANOVA, multiple comparisons test. Error bars indicate SEM). B, brain. E, eye.

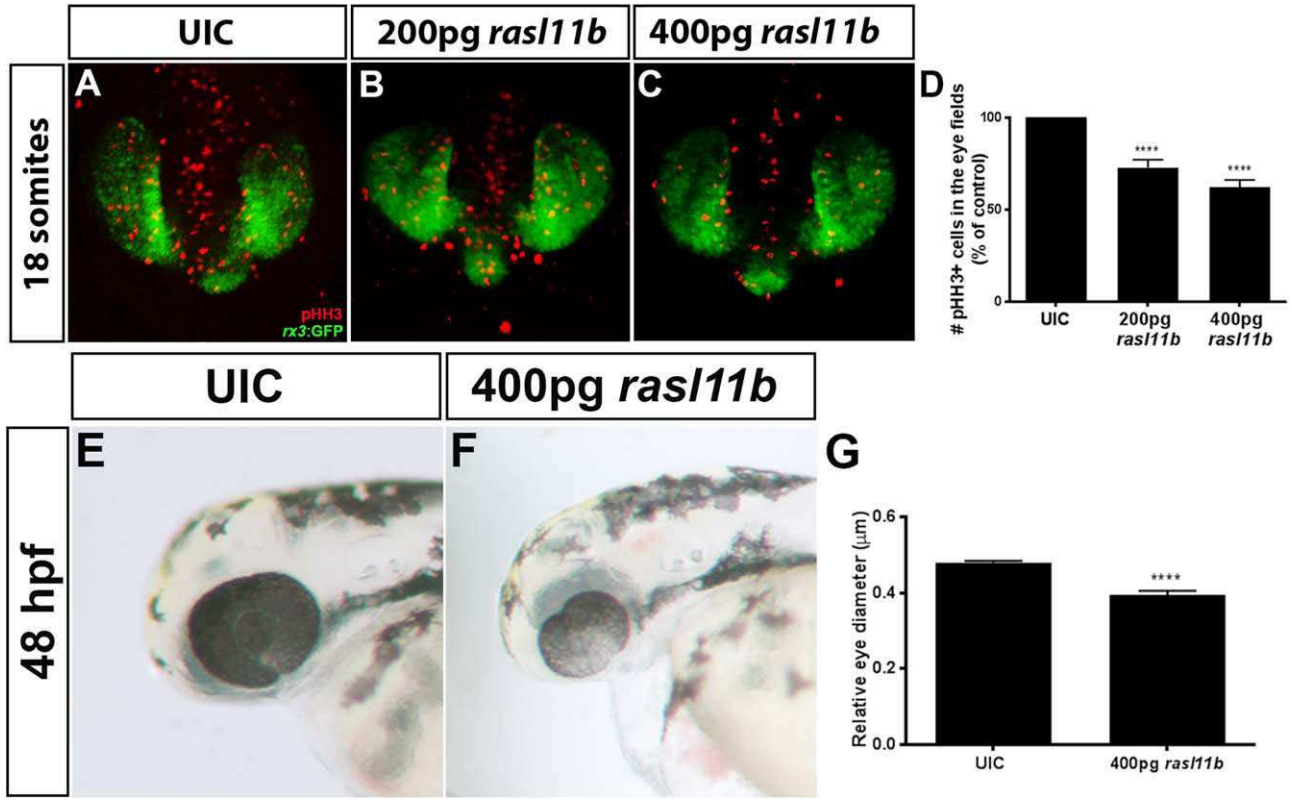

Fig. 5. Overexpression of rasl11b decreases proliferation of RPCs. **A–C:** Confocal dorsal views of 18 somite rx3:GFP embryos co-labeled with pHH3. **D:** Increasing doses of rasl11b resulted in decreased proliferation within the GFP positive eye field (control 100%, N = 3, n = 30; 200 pg rasl11b 72.87% ± 4.25% N = 3, n = 38, ****$P < 0.0001$; 400 pg rasl11b 62.19% ± 4.01%, N = 3, n = 31, ****$P < 0.0001$; one-way ANOVA, multiple comparisons test; error bars indicate SEM). **E–G:** Overexpression of rasl11b results in smaller eyes at 48 hpf (eye diameter relative to head length; control 0.48 μm ± 0.005 μm N = 3, n = 30; 400 pg rasl11b 0.39 μm ± 0.01 μm, N = 3, n = 36; ****$P < 0.0001$; one-way ANOVA, multiple comparisons test; error bars indicate SEM).

for cell migration. Alternatively, increases in MMP2 at the leading edge of migrating RPCs could allow for the ease of pseudopodia through surrounding tissue and cause RPCs to over-migrate.

Conclusions

We confirm through morpholino knockdown, that Sema6A/PlxnA2 signaling regulates proliferation and cohesive migration of RPCs in developing optic vesicles in zebrafish. Here, we provide a resource of genes that are transcriptionally regulated downstream of Sema6A/PlxnA2 signaling. Initial characterization of one gene, *rasl11b*, uncovered its contributing role to the proliferation of RPCs, providing insight into the mechanisms that control this key developmental process. The broadness of Sema/Plxn signaling is only just becoming widely appreciated, and further research into downstream targets and signal propagation is necessary to fully understand the diverse roles of this signaling pair.

Experimental Procedures

Zebrafish Husbandry

*rx3:*GFP zebrafish embryos were generously provided by Jochen Wittbrodt, University of Heidelberg, Germany and developmentally staged as previously described (Kimmel et al., 1995). All procedures were approved by the University of Vermont Institutional Animal Care and Use Committee (IACUC).

Injections and Rescue Constructs

MOs (Gene Tools, Philomath, OR), or mRNA were injected at the one-cell stage (Kimmel et al., 1995). Morpholino concentrations and sequences were as follows: *plxnA2* e2i2, 2 ng (AAAAGCGATGTCTTTCTCACCTTCC); *sema6A*, 4 ng (TGCTGATATCCTGCACTCACCTCAC). Both *sema6A* and *plxnA2* morpholino constructs have been previously validated using RT-PCR to show successful knockdown (Ebert et al., 2014). Off target effects and specificity of morpholinos was addressed by rescue by full length human mRNA and co-injection of *sema6A* or *plxnA2* and *p53* morpholino. Second nonoverlapping morpholino constructs reproduced the same phenotypes, see Ebert et al. (2014). Capped and tailed full-length mRNA, (mMESSAGE mMACHINE kit, Ambion, Austin, TX, cat# AM1344; Poly(A) tailing kit, Invitrogen Cat# AM1350) was generated from plasmids containing human *plxnA2* (Origene, Cat# RC221024) or *sema6A* (Invitrogen, Cat# MDR1734-202803771) and injected into embryos at the one cell stage for a final concentration of 200pg or 400pg/embryo. Full-length, zebrafish *rasl11b* mRNA was generated from pCS2+-DR-Rasl11b generously provided by Dr. Philippe Mourrain (Paris, France).

TABLE 2. Primer Sequences and Accession Numbers Used for Antisense Riboprobe Generation and RT-PCR

Name	Forward primer	Reverse primer	Accession #
rasl11b	ATGCGTCTGATCCAGAACATG	TAATACGACTCACTATAGGGGT CACACTGAAGTGACGGTGC	NM_200140.1
dcdc2b	TGCTTCGTACTGGAGCTGTG	TGCTTCGTACTGGAGCTGTG	NM_001037689.2
shtn-1	TTTAGGTGACACTATAGAAGA GAGGCCTTACGGAAGCTGAAT	TAATACGACTCACTATAGGGGAG ATGCCCAAGAGCTTCTTTTGT	NM_001198761.1
rbl2	TTTAGGTGACACTATAGAAGGG AGATCAAACCCTTCGCTCTG	TAATACGACTCACTATAGGGGAGA AAGAAGCCGTTGATCAGCAT	XM_002666954.5
mmp2	TTTAGGTGACACTATAGAAGGG CCCTTCAAATTCTTGGGTGA	TAATACGACTCACTATAGGGGAGA CAATTTTCTCCGGAAGCTCA	NM_198067.1

Microarray Assay

Uninjected control, *sema6A* morphant, and *plxnA2* morphant embryos were staged at 18 somites and total RNA was isolated from 100 embryos using TRIzol (Invitrogen) followed by ethanol precipitation. Each treatment had four replicates generated from separate injection experiments. Data collection and analyses performed by the IBEST Genomics Resources CORE at the University of Idaho was supported by grants from the National Center for Research Resources (P30GM103324) and the National Institute of General Medical Sciences (8 P20 GM103397-10) from the National Institutes of Health. RNA from 18 somite stage control, *sema6A* and *plxnA2* morphant embryos was analyzed using the NimbleGen Zebrafish 12 × 135 k Array based on Zv9 [090818_Zv7_EXPR], following the NimbleGen arrays user's guide version 5.1.

Microarray Data Analysis

NimbleScan software (NimbleGen. Madison, WI) was used to align a chip-specific grid to control features and extract raw intensity data for each probe and each array. Chip images were then visually checked for each array and verified not to contain any significant spatial artifacts. Raw intensity data was then read into the R statistical computing environment and checked for quality. Chip intensity distributions, boxplots, and hierarchical clusters were compared and checked for any unusual global patterns. Each array was then background corrected and normalized using the quantile normalization procedure and finally each probeset was summarized using the median polish procedure as described with the robust multichip average (RMA) procedure (Irizarry et al., 2003a,b; Bolstad et al., 2003). The median polish procedure is a robust method for summarizing all probes contained within each probeset to a single expression value for each gene, taking into account individual probe effects. Probesets with low levels of expression variation across all samples (interquartile range < 0.5) were removed from further analysis, reducing the overall number of statistical tests to be performed. Differential expression was then assessed using a linear model with an empirical Bayesian adjustment to the variances (Smyth, 2005) and comparisons of interest were extracted using contrasts. The Benjamini and Hochberg (BH) method was used to control for the expected false discovery rate given multiple tests (Benjamini and Hochberg, 1995). Probesets were considered statistically differentially expressed with a BH adjusted P-value of < 0.05. Both raw intensity data (.pair files) and RMA-normalized expression values are available in the National Center for Biotechnology Information Gene Expression Omnibus database (NCBI GEO accession no. GSE86246).

Whole-Mount In Situ Hybridization

Zebrafish embryos were staged at 18 somites, fixed in 4% paraformaldehyde overnight at 4°C, and stored at -20°C in 100% methanol until use. In situ hybridization was performed as described previously (Thisse and Thisse, 2008). DIG-labeled antisense RNA probes were generated using primers listed in Table 2 (IDT, Coralville, IA). PCR products were cloned into pCR 2.1 TOPO vector (Invitrogen, Carlsbad, CA) and sequencing at the UVM Cancer Center Advanced Genome Technologies Core, Burlington, VT. Embryos were oriented in 4% methyl cellulose on depression slides and imaged using a Nikon SMZ800 dissecting light microscope at 50× magnification.

RT-PCR

cDNA was synthesized using SuperScript II reverse transcriptase (Invitrogen) from isolated control, *plxnA2* morphant or *sema6A* morphant total RNA (described above). Gene specific primers (Table 2) were used to amplify approximately 500 base pair amplicons in 10 μl PCR reactions from 1 μg cDNA using PCR Mastermix (Thermo). *ef1α* primers were used as parallel control reactions. PCRs were run on a 1% agarose gel (Invitrogen). Gels were imaged using a Syngene INGENIUS3 system and GENEsys V1.5.5.0 imaging software. Densitometry was performed using Adobe Photoshop CS6. Band intensities were normalized to background, and a ratio of gene band intensity to *ef1α* control levels was obtained for each sample. At least three independent replicates were averaged. Graphs and statistical analyses were obtained using Prism 6.

Sectioning, Imaging, Cell Counts, and Eye Measurements

Embryos were dehydrated in 100% ETOH for 30 min before embedding using a JB4 Embedding Kit (Polysciences, Inc., Warrington, PA) and sectioned on a Leica RM2265 microtome at 20 μm. Brightfield images were obtained using an Olympus iX71 inverted light microscope and figures were assembled using Adobe Photoshop CS6, in which image brightness and contrast were optimized. Eye size measurements were obtained using SPOT imaging software version 5.2. To control for any changes

in overall embryo size, eye size was calculated as a ratio of eye diameter divided by the distance from the anterior tip of the head to the posterior otic placode for each embryo. Proliferating cell counts were recorded when pHH3 positive cells were seen within GFP positive optic vesicles only. For confocal imaging, embryos were mounted in 0.5% low-melt agarose on glass bottom dishes (CLS-1811 ChemGlass, NJ) and imaged at 20× using 2-μm steps on a Nikon Eclipse Ti inverted microscope. Z Stacks were subjected to a Kalman stack filter in Image J and were presented as maximum intensity projections. RGB images were generated in Adobe Photoshop CS6.

Whole-Mount Immunohistochemistry

Eighteen somite stage embryos were fixed in 4% paraformaldehyde overnight at 4°C, rehydrated in PBST (phosphate buffered saline + 1% Triton), incubated in immuno block (PBST + 10% normal goat serum) for 1 hr at room temperature, primary antibody in immuno block overnight at 4°C, secondary antibody for 2 hr at room temperature and stored in PBST until imaged. Antibodies used: phospho-Histone H3, pHH3 (1:1,000, Cell Signaling, Cat# 3377, Danvers, MA), anti-rabbit Alexa Flour 555 (1:1,000, Cell Signaling, Cat# 4413S).

Acknowledgments

VGN Bioinformatics Core services were supported by an Institutional Development Award (IDeA) from the National Institute of General Medical Sciences of the National Institutes of Health under grant number P20GM103449. Its contents are solely the responsibility of the authors and do not necessarily represent the official views of NIGMS or NIH. Thank you to Dr. Paula Deming, Department of Nuclear Medicine and Radiological Sciences, University of Vermont for guidance and insight. Authors have no conflict of interest to declare.

References

Behar O, Golden JA, Mashimo H, Schoen FJ, Fishman MC. 1996. Semaphorin III is needed for normal patterning and growth of nerves, bones and heart. Nature 383:525–528.

Belle M, Parray A, Belle M, Chedotal A, Nguyen-Ba-Charvet KT. 2016. PlexinA2 and Sema6A are required for retinal progenitor cell migration. Dev Growth Differ 58:492–502.

Benjamini Y, Hochberg Y. 1995. Controlling the false discovery rate: a practical and powerful approach to multiple testing. J R Stat Soc Series B Stat Methodol 57:289–300.

Bolstad BM, Irizarry RA, Astrand M, Speed TP. 2003. A comparison of normalization methods for high density oligonucleotide array data based on variance and bias. Bioinformatics 19:185–193.

Bos JL, Rehmann H, Wittinghofer A. 2007. GEFs and GAPs: Critical elements in the control of small G proteins. Cell 129:865–877.

Brinckerhoff CE, Matrisian LM. 2002. Matrix metalloproteinases: a tail of a frog that became a prince. Nat Rev Mol Cell Biol 3:207–214.

Cobrinik D. 2005. Pocket proteins and cell cycle control. Oncogene 24:2796–2809.

Colicelli J. 2004. Human RAS superfamily proteins and related GTPases. Science's STKE 2004:RE13.

Dijkmans TF, van Hooijdonk LW, Fitzsimons CP, Vreugdenhil E. 2010. The doublecortin gene family and disorders of neuronal structure. Cent Nerv Syst Agents Med Chem 10:32–46.

Dingar D, Konecny F, Zou J, Sun X, von Harsdorf R. 2012. Anti-apoptotic function of the E2F transcription factor 4 (E2F4)/p130, a member of retinoblastoma gene family in cardiac myocytes. J Mol Cell Cardiol 53:820–828.

Ebert AM, Childs SJ, Hehr CL, Cechmanek PB, McFarlane S. 2014. Sema6a and Plxna2 mediate spatially regulated repulsion within the developing eye to promote eye vesicle cohesion. Development 141:2473–2482.

Friend SH, Bernards R, Rogelj S, Weinberg RA, Rapaport JM, Albert DM, Dryja TP. 1986. A human DNA segment with properties of the gene that predisposes to retinoblastoma and osteosarcoma. Nature 323:643–646.

Ganguly A, Yang H, Sharma R, Patel KD, Cabral F. 2012. The role of microtubules and their dynamics in cell migration. J Biol Chem 287:43359–43369.

Grati Mh, Chakchouk I, Ma Q, Bensaid M, Desmidt A, Turki N, Yan D, Baanannou A, Mittal R, Driss N, Blanton S, Farooq A, Lu Z, Liu XZ, Masmoudi S. 2015. A missense mutation in DCDC2 causes human recessive deafness DFNB66, likely by interfering with sensory hair cell and supporting cell cilia length regulation. Hum Mol Genet 24:2482–2491.

He H, Yang T, Terman JR, Zhang X. 2009. Crystal structure of the plexin A3 intracellular region reveals an autoinhibited conformation through active site sequestration. Proc Natl Acad Sci U S A 106:15610–15615.

Irizarry RA, Bolstad BM, Collin F, Cope LM, Hobbs B, Speed TP. 2003a. Summaries of affymetrix GeneChip probe level data. Nucleic Acids Res 31:e15.

Irizarry RA, Hobbs B, Collin F, Beazer-Barclay YD, Antonellis KJ, Scherf U, Speed TP. 2003b. Exploration, normalization, and summaries of high density oligonucleotide array probe level data. Biostatistics 4:249–264.

Kimmel CB, Ballard WW, Kimmel SR, Ullmann B, Schilling TF. 1995. Stages of embryonic development of the zebrafish. Dev Dyn 203:253–310.

Lai A, Kennedy BK, Barbie DA, Bertos NR, Yang XJ, Theberge M-C, Tsai S-C, Seto E, Zhang Y, Kuzmichev A, Lane WS, Reinberg D, Harlow E, Branton PE. 2001. RBP1 recruits the mSIN3-histone deacetylase complex to the pocket of retinoblastoma tumor suppressor family proteins found in limited discrete regions of the nucleus at growth arrest. Mol Cell Biol 21:2918–2932.

Lemmens K, Bollaerts I, Bhumika S, De Groef L, Van Houcke J, Darras VM, Van Hove I, Moons L. 2016. Matrix metalloproteinases as promising regulators of axonal regrowth in the injured adult zebrafish retinotectal system. J Comp Neurol 524:1472–1493.

Louro R, Nakaya HI, Paquola AC, Martins EA, da Silva AM, Verjovski-Almeida S, Reis EM. 2004. RASL11A, member of a novel small monomeric GTPase gene family, is down-regulated in prostate tumors. Biochem Biophys Res Commun 316:618–627.

Luo Y, Raible D, Raper JA. 1993. Collapsin: A protein in brain that induces the collapse and paralysis of neuronal growth cones. Cell 75:217–227.

Murphree AL, Benedict WF. 1984. Retinoblastoma: clues to human oncogenesis. Science 223:1028.

Negishi M, Oinuma I, Katoh H. 2005. Plexins: axon guidance and signal transduction. Cell Mol Life Sci 62:1363–1371.

Neufeld G, Kessler O. 2008. The semaphorins: versatile regulators of tumour progression and tumour angiogenesis. Nat Rev Cancer 8:632–645.

Oinuma I, Ishikawa Y, Katoh H, Negishi M. 2004. The semaphorin 4D receptor plexin-B1 is a GTPase activating protein for R-Ras. Science 305:862–865.

Pasterkamp RJ. 2005. R-Ras fills another GAP in semaphorin signalling. Trends Cell Biol 15:61–64.

Pezeron G, Lambert G, Dickmeis T, Strahle U, Rosa FM, Mourrain P. 2008. Rasl11b knock down in zebrafish suppresses one-eyed-pinhead mutant phenotype. PLoS One 3:e1434.

Rembold M, Loosli F, Adams RJ, Wittbrodt J. 2006. Individual cell migration serves as the driving force for optic vesicle evagination. Science 313:1130–1134.

Renaud J, Chedotal A. 2014. Time-lapse analysis of tangential migration in Sema6A and PlexinA2 knockouts. Mol Cell Neurosci 63:49–59.

Renaud J, Kerjan G, Sumita I, Zagar Y, Georget V, Kim D, Fouquet C, Suda K, Sanbo M, Suto F, Ackerman SL, Mitchell KJ,

Fujisawa H, Chedotal A. 2008. Plexin-A2 and its ligand, Sema6A, control nucleus-centrosome coupling in migrating granule cells. Nat Neurosci 11:440–449.

Rünker AE, Little GE, Suto F, Fujisawa H, Mitchell KJ. 2008. Semaphorin-6A controls guidance of corticospinal tract axons at multiple choice points. Neural Dev 3:34.

Serini G, Valdembri D, Zanivan S, Morterra G, Burkhardt C, Caccavari F, Zammataro L, Primo L, Tamagnone L, Logan M, Tessier-Lavigne M, Taniguchi M, Puschel AW, Bussolino F. 2003. Class 3 semaphorins control vascular morphogenesis by inhibiting integrin function. Nature 424:391–397.

Shi W, Kumanogoh A, Watanabe C, Uchida J, Wang X, Yasui T, Yukawa K, Ikawa M, Okabe M, Parnes JR, Yoshida K, Kikutani H. 2000. The class IV semaphorin CD100 plays nonredundant roles in the immune system: defective B and T cell activation in CD100-deficient mice. Immunity 13:633–642.

Shimada T, Toriyama M, Uemura K, Kamiguchi H, Sugiura T, Watanabe N, Inagaki N. 2008. Shootin1 interacts with actin retrograde flow and L1-CAM to promote axon outgrowth. J Cell Biol 181:817–829.

Smyth GK. 2005. limma: linear models for microarray data. In: Gentleman R, Carey VJ, Huber W, Irizarry RA, Dudoit S, editors. Bioinformatics and computational biology solutions using R and bioconductor. New York, NY: Springer New York; p 397–420.

Tamagnone L, Artigiani S, Chen H, He Z, Ming GI, Song H, Chedotal A, Winberg ML, Goodman CS, Poo M, Tessier-Lavigne M, Comoglio PM. 1999. Plexins are a large family of receptors for transmembrane, secreted, and GPI-anchored semaphorins in vertebrates. Cell 99:71–80.

Tawarayama H, Yoshida Y, Suto F, Mitchell KJ, Fujisawa H. 2010. Roles of semaphorin-6B and plexin-A2 in lamina-restricted projection of hippocampal mossy fibers. J Neurosci 30:7049–7060.

Thisse C, Thisse B. 2008. High-resolution in situ hybridization to whole-mount zebrafish embryos. Nat Protoc 3:59–69.

Toriyama M, Shimada T, Kim KB, Mitsuba M, Nomura E, Katsuta K, Sakumura Y, Roepstorff P, Inagaki N. 2006. Shootin1: a protein involved in the organization of an asymmetric signal for neuronal polarization. J Cell Biol 175:147–157.

Toyofuku T, Yoshida J, Sugimoto T, Zhang H, Kumanogoh A, Hori M, Kikutani H. 2005. FARP2 triggers signals for Sema3A-mediated axonal repulsion. Nat Neurosci 8:1712–1719.